

Chapter 5

Kinetics of Ruthenacyclobutanes Related to Degenerate Metathesis

The text in this chapter is reproduced in part with permission from:

Keitz, B. K.; Grubbs, R. H. *J. Am. Chem. Soc.* **2011**, 133, 16277.

Copyright 2011 American Chemical Society

Abstract

The preparation of new phosphonium alkylidene ruthenium metathesis catalysts containing N-heterocyclic carbenes (NHCs) that result in a preference for degenerate metathesis is described. The reaction of these catalysts with ethylene or substrates relevant to ring-closing metathesis (RCM) produced ruthenacyclobutanes that could be characterized by cryogenic NMR spectroscopy. The rate of α/β methylene exchange in ethylene-only ruthenacycles was found to vary widely between ruthenacycles, in some cases being as low as 3.97 s^{-1} at $-30 \text{ }^\circ\text{C}$, confirming that the NHC plays an important role in degenerative metathesis reactions. Attempts to generate RCM-relevant ruthenacycles resulted in the low-yielding formation of a previously unobserved species, which we assign as a β -alkyl substituted ruthenacycle. Kinetic investigations of the RCM-relevant ruthenacycles in the presence of excess ethylene revealed a large increase in the kinetic barrier of the rate-limiting dissociation of the cyclopentene RCM product compared to previously investigated catalysts. Taken together, these results shed light on the degenerate/productive selectivity differences observed between different metathesis catalysts.

Introduction

As discussed in Chapter 4, implicit in many olefin metathesis reactions is the presence of degenerate or nonproductive events. For instance, in the cross-metathesis reaction of propylene, a productive reaction would result in the formation of 2-butene, while a degenerate reaction would reform propylene. As the

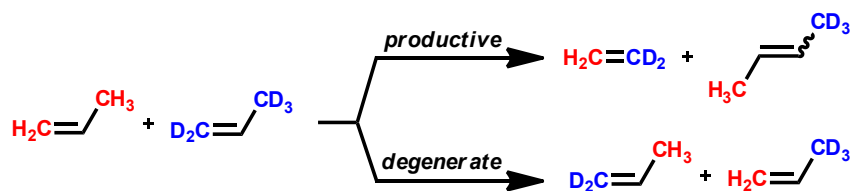


Figure 5.1. Productive and degenerate metathesis of propylene

degenerate reaction reproduces the starting olefin, it can only be reliably studied via isotopic cross-over experiments (Figure 5.1). In Chapter 4, we reported on the study of degenerate events taking place during the ring-closing metathesis (RCM) of an isotopically labeled diethyl diallylmalonate (**5.1**) and discovered the surprising effect of NHC structure on a catalysts propensity to perform either productive or degenerate turnovers (TON).¹ The results of this study validated the importance of degenerate metathesis events and their subsequent effect on catalyst stability and efficiency. We also established that selectivity for degenerate metathesis may actually be beneficial in some applications, such as the ethenolysis of methyl oleate.²

For ruthenium metathesis catalysts, the effect of ligand structure on initiation and stability has been well documented.^{3,4} This information has allowed for the development of increasingly sophisticated catalysts. However, much less is known about the effect of ligand structure on processes that occur within a complex catalytic cycle such as RCM. This lack of understanding has made it difficult to rationalize the behavior of catalysts asked to conduct increasingly challenging transformations. Recently, the situation has been remedied by the development of rapidly initiating catalysts and their ability to efficiently form ruthenacyclobutanes at low temperature, which has facilitated the solution-phase study of previously inaccessible metathesis intermediates by our group⁵ as well as Piers and co-workers

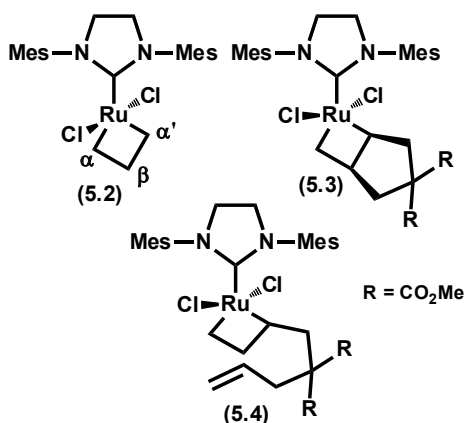


Figure 5.2. Previously observed ruthenacycles relevant to RCM

(Figure 5.2).^{6,7} By analyzing these intermediates and through a combination of kinetics and kinetic modeling, the Piers laboratory has been able to determine the activation energies for the fundamental steps along a productive RCM pathway.⁸

While the above results will undoubtedly facilitate the development of more efficient catalysts, we sought to utilize them as a basis to establish the effect of the NHC on each elementary reaction in the RCM catalytic cycle. Specifically, we wanted to correlate these effects with preference for degenerate selectivity and thereby acquire a more intimate understanding of the role of the NHC in establishing the selectivity for either degenerate or productive olefin metathesis. In this chapter, we report our progress towards this goal.

Results and Discussion

Considering our interest in degenerate metathesis, catalysts incorporating NHCs known to give lower selectivity for productive metathesis in the RCM of **5.1** were selected for study.¹ Thus, we started with previously reported catalyst **5.5** and performed a phosphine exchange in order to expedite the formation of

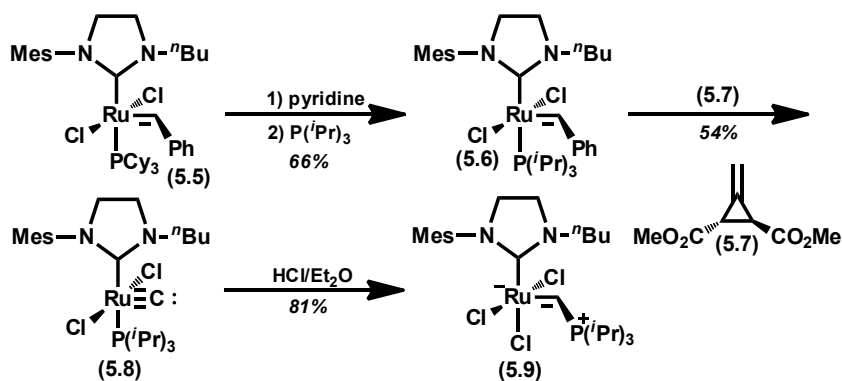


Figure 5.3. Synthesis of phosphonium alkylidene catalyst **5.9**

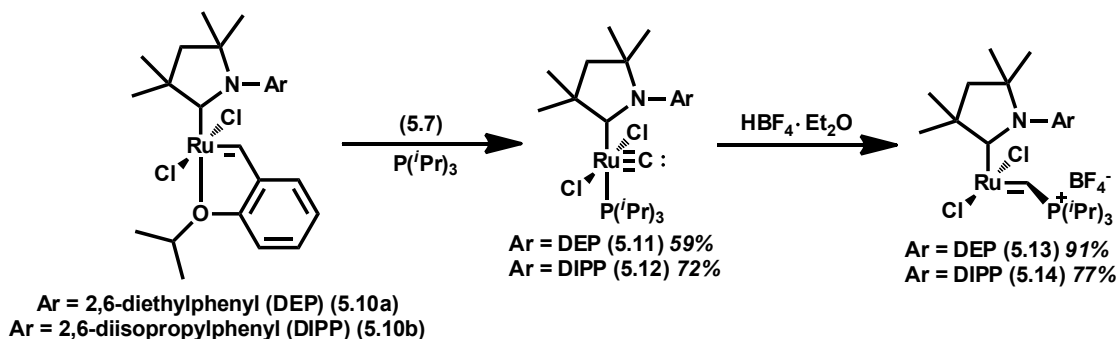


Figure 5.4. Synthesis of catalysts **5.13** and **5.14**

ruthenacycles.^{6,9} Subsequent reaction with Feist's ester (**5.7**) yielded carbide **5.8**, which was then protonated with HCl in Et₂O to afford the desired phosphonium alkylidene complex **5.9** in good yield (Figure 5.3).^{10,11}

Similarly, reaction of the cyclic alkylamino carbene (CAAC) catalysts of type **5.10** with **5.7** in the presence of 1 equivalent of P(iPr)₃ yielded carbides **5.11** and **5.12** which were then protonated in a manner analogous to **5.8** to obtain the desired complexes (**5.13** and **5.14**, Figure 5.4). It should be noted that, this result demonstrates that phosphonium alkylidene complexes may be obtained from Hoveyda-type parent complexes in situations where the corresponding phosphine precursor is synthetically inaccessible.

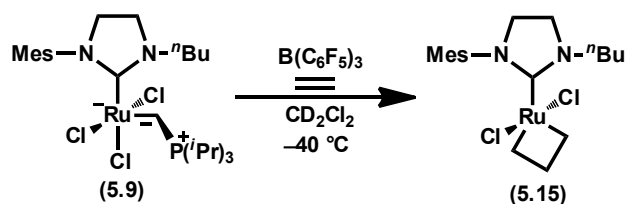


Figure 5.5. Generation of ethylene-only ruthenacycles from **5.9**

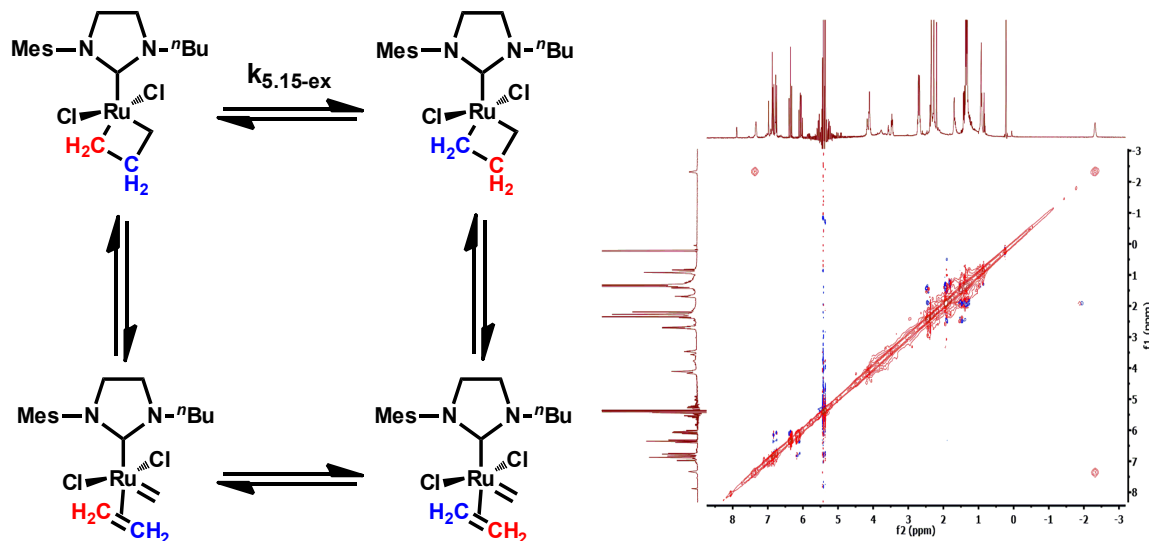


Figure 5.6. Mechanism of ruthenacycle methylene exchange (left) and ROESY spectrum at -60 °C with cross-peaks indicative of chemical exchange (right)

With **5.9**, **5.13**, and **5.14** in hand, we next attempted the preparation of ethylene-derived ruthenacycles, as even these simple metallacycles can provide insight into the influence of the NHC ligand. Gratifyingly, complete conversion to metallacycle **5.15** was observed after 3 h at -40 °C when **5.9** was exposed to $\text{B}(\text{C}_6\text{F}_5)_3$ and 1 atm of ethylene (Figure 5.5). Consistent with analogous complexes, **5.15** displayed an upfield resonance at $\delta = -2.4$ ppm characteristic of the hydrogen on the β -carbon of the ruthenacycle. We found compound **5.15** to be stable for several days at -78 °C and it could be fully characterized by $^1\text{H-NMR}$ spectroscopy and 2D techniques such as $^1\text{H-}^1\text{H}$ COSY (see Experimental section).¹² A ROESY

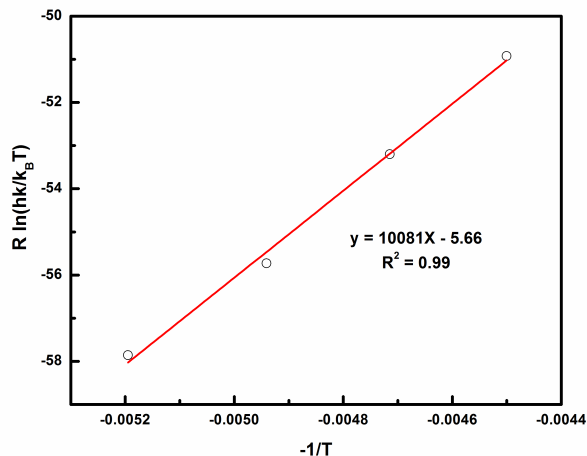


Figure 5.7. Eyring plot for ruthenacycle methylene exchange in **5.15**

spectrum taken at $-60\text{ }^{\circ}\text{C}$ (Figure 5.6) displayed cross-peaks indicative of chemical exchange between the protons on the α and β carbons of the ruthenacycle. Curiously, cross-peaks were only observed between α -H and β -H and not between α' -H and β -H. Although interesting, this situation is not unprecedented, and appears to be a result of asymmetry in the NHC affecting the ruthenacycle.⁵ We next attempted to measure the rate of exchange ($k_{5.15\text{-Ex}}$) between α and β protons using exchange spectroscopy (EXSY). Unfortunately, the presence of a minor peak overlapping with the α -H resonance in **5.15** resulted in irreproducible measurements. However, switching to a magnetization transfer technique allowed us to obtain a $k_{5.15\text{-Ex}}$ of 10.5 s^{-1} at $-60\text{ }^{\circ}\text{C}$ (see Experimental).¹³ This rate is in good agreement with previous reports of ruthenacycles incorporating H_2IMes ($\text{H}_2\text{IMes} = 1,3\text{-dimesitylimidazolidine-2-ylidene}$) such as **5.2**. An Eyring plot (Figure 5.7) from $-40\text{ }^{\circ}\text{C}$ to $-80\text{ }^{\circ}\text{C}$ yielded values for ΔH^{\ddagger} and ΔS^{\ddagger} of $10.1 \pm 0.5\text{ kcal mol}^{-1}$ and $-5.7 \pm 2.2\text{ cal mol}^{-1}\text{ K}^{-1}$, respectively.

Similar to the case of **5.9** above, the reactions of **5.13** and **5.14** with an

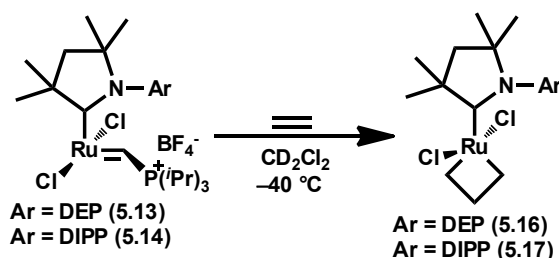


Figure 5.8. Generation of ethylene-only ruthenacycles from **5.13** and **5.14**

Table 5.1. Ruthenacycle methylene exchange rates for all complexes

Complex	Temperature, °C	α/β methylene exchange rate, s ⁻¹
5.15	-60	10.5
5.16	-30	3.97
5.17	-60	1.48

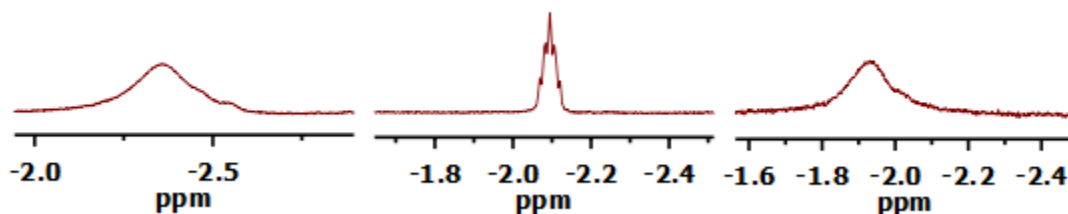


Figure 5.9. ¹H NMR spectrum of β -H ruthenacycles resonance for **5.15** (left), **5.16** (middle), and **5.17** (right) at -30 °C in CD₂Cl₂

excess of ethylene under similar conditions cleanly yielded ruthenacycles **5.16** and **5.17** (Figure 5.8).¹⁴ Characterization of **5.16** was performed according to the same procedure described above, but a ROESY NMR spectrum at -60 °C showed only an NOE between the α -H and β -H; no evidence of chemical exchange was observed. In fact, chemical exchange via ROESY and magnetization transfer was not observed until the temperature was raised to -30 °C! Measurement of the

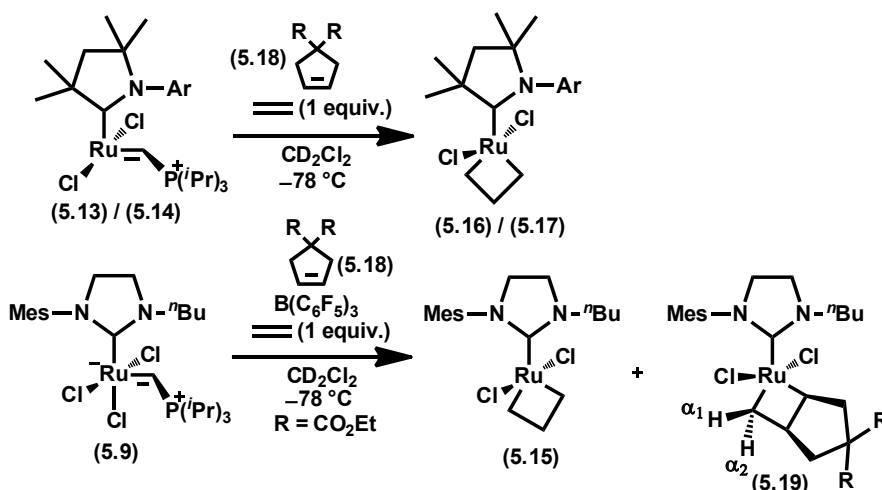


Figure 5.10. Synthesis of substituted ruthenacycles from **5.9** and **5.13**

exchange rate via magnetization transfer yielded an extraordinarily low value of 3.97 s^{-1} at $-30 \text{ }^\circ\text{C}$ (Table 5.1). Thus, compared with other catalysts (e.g., **5.2** and **5.15**), $k_{5.16\text{-Ex}}$ is lower, even at higher temperatures. This effect can be qualitatively observed: the ruthenacycle resonances in **5.16** were still sharp at $-30 \text{ }^\circ\text{C}$ whereas the same resonances in **5.15** were significantly broadened as a result of chemical exchange (Figure 5.9). In contrast to **5.16**, a ROESY NMR spectrum of ruthenacycle **5.17** taken at $-60 \text{ }^\circ\text{C}$ showed evidence of chemical exchange, albeit with a relatively low rate constant (Table 5.1). Although it is difficult to extract definitive conclusions based on such dramatic changes in methylene exchange rates, particularly at the low temperatures under investigation, the extent to which the NHC can affect even the simplest of metathesis reactions is still noteworthy. Furthermore, the low rate of exchange of **5.16**, even at relatively high temperatures, suggests that similar complexes may be viable targets for crystallographic characterization of metathesis-relevant ruthenacycles.

Having established the feasibility of forming simple ruthenacycles with **5.9**,

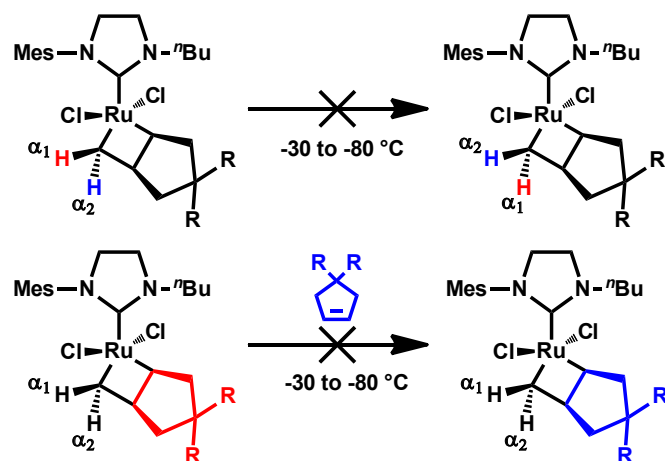


Figure 5.11. Unobserved exchange processes in **5.19**

5.13, and **5.14**, we turned to the preparation and characterization of ruthenacycles relevant to RCM. Adopting a similar approach to the Piers' laboratory, **5.9**, **5.13**, and **5.14** were reacted with the cyclopentene product (**5.18**) resulting from the RCM of diethyl diallylmalonate (**5.1**) in the presence of $B(C_6F_5)_3$ and 1 equiv. of ethylene (Figure 5.10).^{6,8} Unfortunately, under a variety of conditions, both **5.13** and **5.14** reacted to give the ethylene-only ruthenacycles **5.16** and **5.17**, respectively. Such an observation is consistent with the known preference of catalysts containing these NHCs to propagate as methyldiene species in catalytic reactions (e.g., in ethenolysis),¹⁵ but it is nevertheless surprising that no other ruthenacycles were observed.¹⁶ In contrast to **5.13** and **5.14**, when **5.9** was reacted with **5.15** and 1 equiv. of ethylene at $-78\text{ }^\circ\text{C}$, substituted metallacycle **5.19** was observed, albeit in very low yield (ca. 29%). In all cases, a significant amount of the parent ethylene-only metallacycle **5.15** was also formed (ca. 21% yield). Despite the low yield of **5.19**, we were able to fully characterize the metallacycle resonances by ^1H - ^1H COSY spectroscopy and found them to be consistent with previous literature

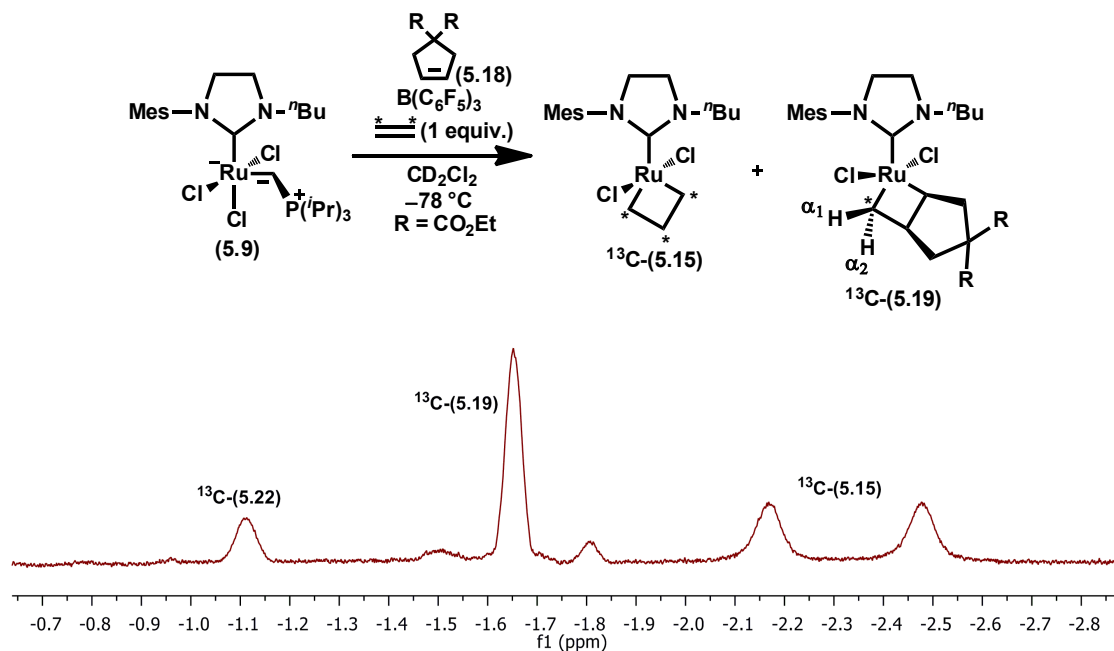


Figure 5.12. Generation of substituted ruthenacycles using ¹³C-ethylene showing ¹³C-(**5.15**) ($\delta = -2.2$ ppm and -2.5 ppm), ¹³C-(**5.19**) ($\delta = -1.65$ ppm), and ¹³C-(**5.22**) ($\delta = -1.1$ ppm)

reports (*vide infra*).^{6,8} To our surprise, ROESY spectra taken at a variety of different temperatures (-40 °C to -70 °C) and mixing times (up to 600 ms) displayed no evidence of chemical exchange apart from the methylene exchange in **5.15**. This is in contrast to compound **5.3**, which exhibits a number of dynamic processes including exchange between α^1 and α^2 resonances and exchange between **5.3** and free cyclopentene (Figure 5.11).

Upon warming the mixture of **5.15** and **5.19** to -40 °C for 2 h, a new peak appeared in the metallacycle region of the NMR spectrum. At first, we believed this peak to be the result of ring opening of **5.19** followed by trapping with ethylene, a process that was observed by Piers (e.g. to form **5.4**).⁸ However, several lines of evidence suggest that, under our conditions, an entirely different intermediate is

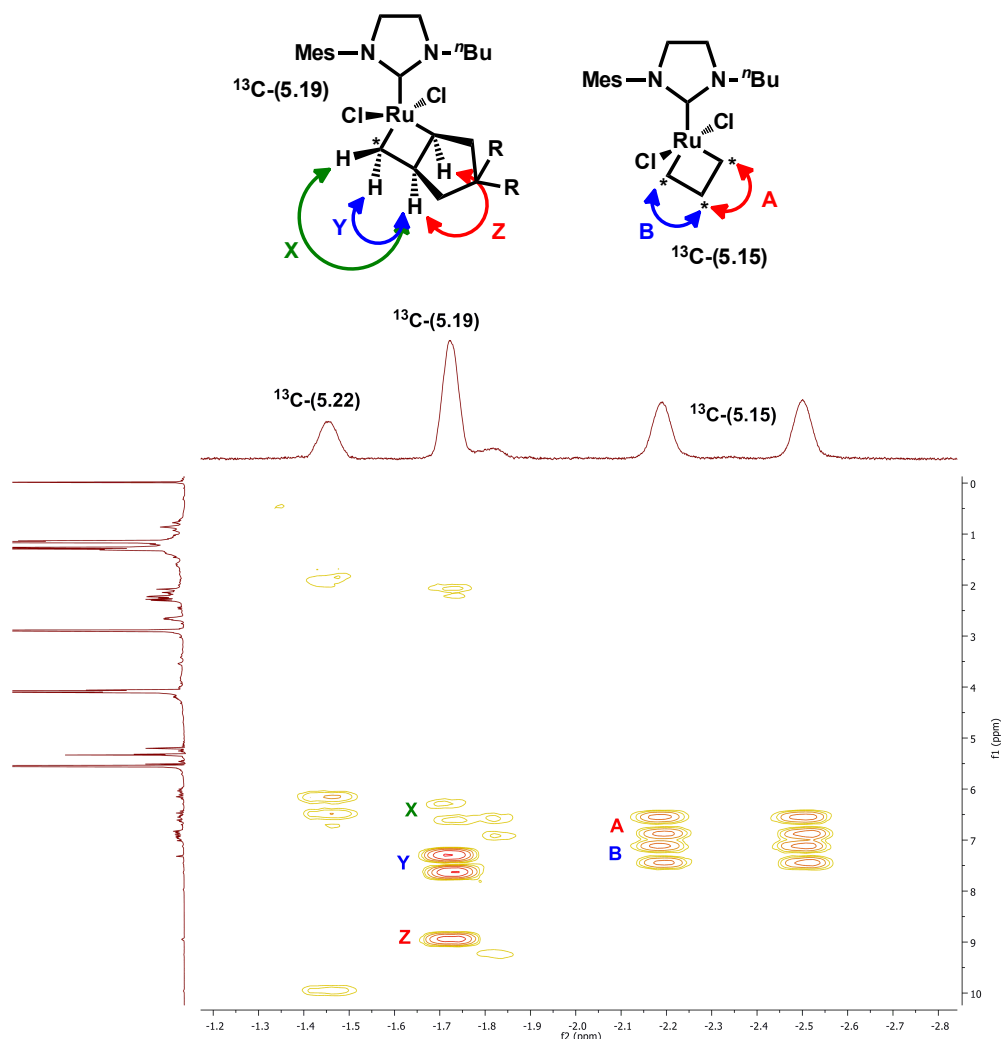


Figure 5.13. ^1H - ^1H COSY of ruthenacycles region for ^{13}C -labelled ruthenacycle mixture at $-90\text{ }^\circ\text{C}$ in CD_2Cl_2 . Note that the assignments of **A** and **B** in ^{13}C -(**5.15**) are arbitrary since there was not enough spectroscopic data to distinguish the two. **X**, **Y**, and **Z** assignments were confirmed by 2D NOESY

formed. First, Piers and coworkers found that ring-opened ruthenacycle **5.4** was only formed at low temperatures (below $-60\text{ }^\circ\text{C}$) whereas the formation of the observed structure only occurred at higher temperatures ($-40\text{ }^\circ\text{C}$). Second and more importantly, substitution at α' should create a set of diastereotopic β -H resonances. Thus, if a structure analogous to **5.4** is correct, there should have been two separate resonances, which were not observed. In order to characterize

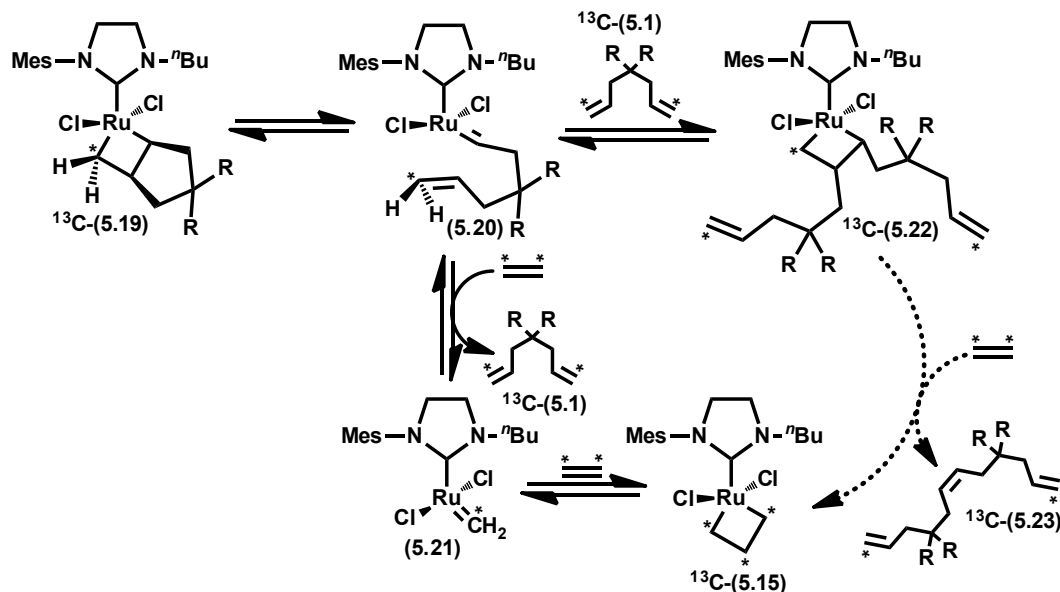


Figure 5.14. Proposed formation of diene **5.1** and ruthenacycles **5.22** from **5.19** and ethylene. Dashed lines represent a possible process that was not observed

this new species and to confirm the identity of **5.19**, compound **5.9** was reacted with **5.18** in the presence of ^{13}C -labelled ethylene (Figure 5.12). The resulting NMR spectrum taken at $-60\text{ }^\circ\text{C}$ showed that only one of the three $\beta\text{-H}$ resonances ($\delta = -2.4\text{ ppm}$) was split by virtue of being bound to a ^{13}C -enriched nucleus.¹⁷ This corresponds to the ethylene-only ruthenacycle **5.15**. The other two $\beta\text{-H}$ resonances remained as singlets, which indicated that these protons must have come from substrate **5.18**. These data rules out the presence of a ruthenacycle resulting from the ring opening of **5.19** and trapping of the resulting alkylidene with ethylene. The extremely low concentration of the unknown ruthenacycle and its relatively short T_2 prevented us from establishing its structure by heteronuclear 2D NMR spectroscopy (e.g., HSQC, HMBC).¹⁸ However, we were able to obtain a ^1H - ^1H COSY spectrum at $-90\text{ }^\circ\text{C}$ that provided some insight into the structure of the unknown species (Figure 5.13). The COSY confirms our original assignment of **5.15** and **5.19** and

also shows cross-peaks for the unknown species that suggest the following : 1) The β -carbon of the ruthenacycle is substituted with an alkyl group, as shown by a small correlation observed in the alkyl region; 2) The β -H is adjacent to a ^{13}C -enriched nucleus which is shown by a correlation in the α/α' -H ruthenacycle region that is split into a doublet; 3) The α -carbon of the ruthenacycle is also alkyl-substituted as shown by a downfield correlation that is consistent with other α -substituted ruthenacycles. Based on these results, we propose structure **5.22** in Figure 5.14 as the unknown ruthenacycle. If this structure is correct, it would be the first observation of a β -substituted ruthenacycle that is not part of a ring system. However, as a caveat, it must be noted that, it is currently not clear what role (if any) a structure such as **5.22** plays in either productive or nonproductive metathesis. The formation of **5.22** would require ring opening of **5.19** to generate an alkylidene followed by trapping with diene ^{13}C -**(5.1)** instead of ethylene (Figure 5.14). This would obviously require that diene ^{13}C -**(5.1)** be present in solution and an HSQC and ^{13}C NMR spectrum confirmed its presence. Unfortunately, we were unable to reliably establish its concentration due to the overlap of several species in the same region of the 1D ^1H NMR spectrum (see the Experimental).¹⁹ However, reaction of **5.9** with diene **5.1** in place of **5.18** yielded the same three ruthenacycle resonances, although the relative concentration of the various ruthenacycles was largely unchanged compared to previous experiments. Structure **5.22** is consistent with all of our spectroscopic data, but unfortunately, its low concentration has prevented us from establishing its identity with full confidence.²⁰ Furthermore, we were also unable to find conditions where **5.22** did not form, a fact that has

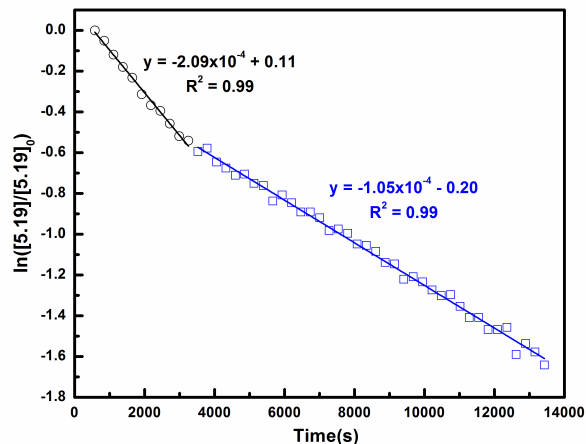


Figure 5.15. Log pot of [5.19] showing two apparent first-order decay processes

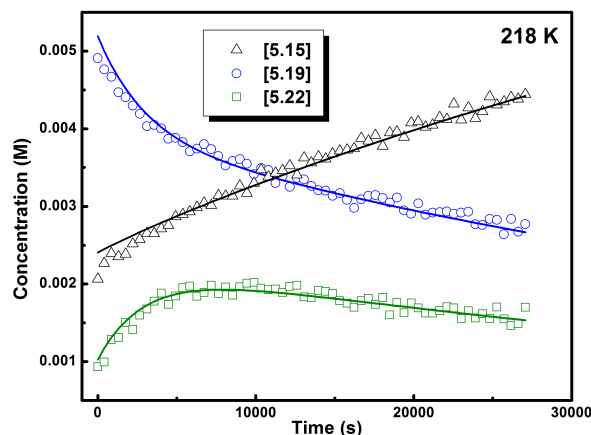


Figure 5.16. Concentration profiles and kinetic fits derived from COPASI for **5.15**, **5.19**, and **5.22** at $-55\text{ }^{\circ}\text{C}$

tremendously complicated our kinetic investigations. Despite these difficulties, we decided to probe the transformation from **5.19** to **5.15**, in the hopes of providing some insight into the effect of the NHC on more advanced ruthenacycle kinetics.

The exposure of an isotopically labeled mixture of ^{13}C -**5.19** and ^{13}C -**5.22** to an excess of ethylene (1 atm) at $-60\text{ }^{\circ}\text{C}$ for 6 hours revealed only a marginal decrease in the intensity of their corresponding resonances. This result is in contrast to what the Piers' laboratory observed with **5.3**, which was consumed

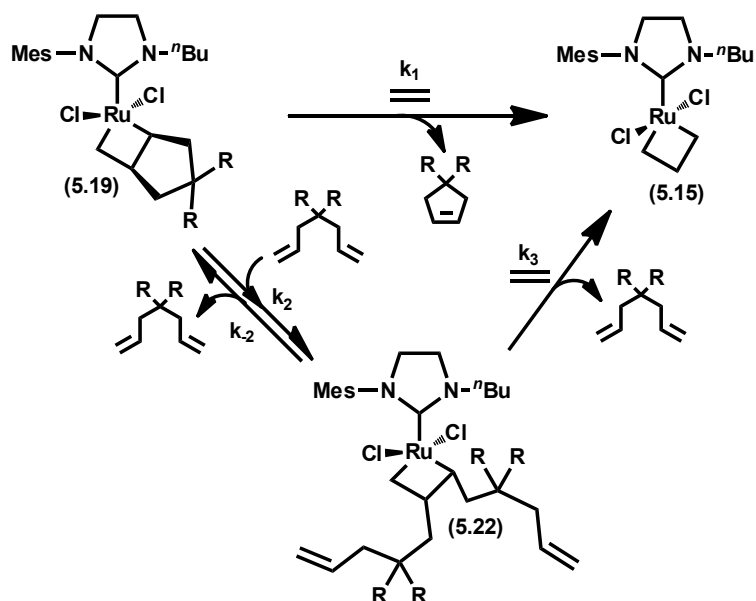


Figure 5.17. Simplified kinetic model for conversion of **5.19** to **5.15** and **5.22** in the presence of excess ethylene

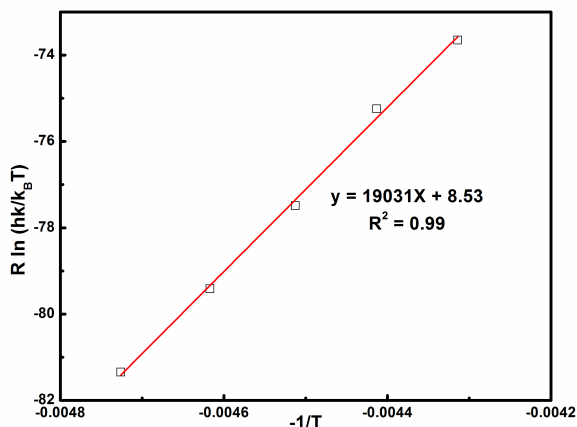


Figure 5.18. Eyring plot for k_1 values (see Figure 5.17) derived from kinetic simulation

within hours under similar conditions. Perhaps more surprising was the slow rate of reaction of ruthenacycle ^{13}C -**5.15**, which showed almost no significant washing out of the ^{13}C label. Again, this is in contrast to catalyst **5.2** formed from ^{13}C -labelled ethylene, where the isotopic label was completely washed out within hours, albeit at the higher temperature of $-50\text{ }^\circ\text{C}$.⁶ In a separate experiment, increasing the

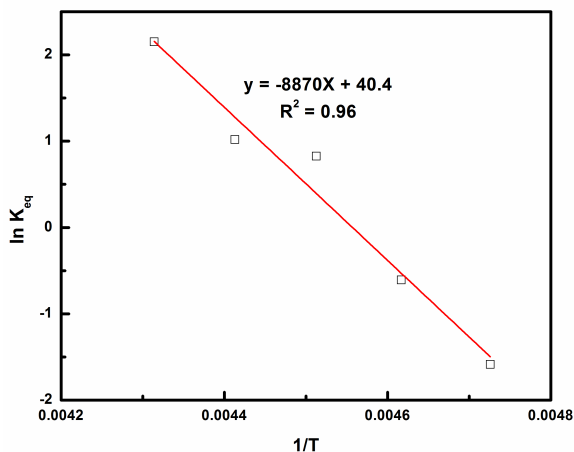


Figure 5.19. Van't Hoff plot using K_{eq} (k_2/k_{-2}) values from COPASI kinetic simulation

temperature of the reaction of **5.19** with excess ethylene to form **5.15** at -40 °C resulted in clean first-order kinetics that could be monitored on a more manageable timeframe using NMR spectroscopy. However, a closer inspection of the kinetic data revealed a second first-order process that appeared to be occurring at short reaction times (Figure 5.15). We believe this additional process was the result of an equilibrium between **5.19** and **5.22** at early reaction times. Indeed, a time course plot of the concentrations of **5.15**, **5.19**, and **5.22** revealed a slight increase in the concentration of **5.22** followed by a leveling off at later reaction times (Figure 5.16). This result confirms that there are two processes leading to the decrease in the concentration of **5.19**: direct reaction to form **5.15** with release of **5.18**, and an apparent equilibrium reaction to form **5.22**, followed by the subsequent conversion of **5.22** into **5.15** (Figure 5.17).²¹ An analogous sequence of reactions was observed by Piers' under certain conditions, albeit with a different intermediate (**5.4**). Modeling of the simplified series of reactions shown in Figure 5.17 using COPASI²² allowed

for the determination of kinetic parameters k_1 , k_2 , k_{-2} , and k_3 (Figure 5.16).^{23,24} Comparing the k_1 values obtained for **5.19** and **5.3**¹⁶ revealed a stark contrast between the reactivity of the two compounds. For example, at -60 °C, the k_1 value obtained for **5.3** was $7 \times 10^{-4} \text{ s}^{-1}$, whereas the value for **5.19** was two orders of magnitude less at $7.3 \times 10^{-6} \text{ s}^{-1}$. An Eyring plot for k_1 values (Figure 5.18) of **5.19** over a 20 °C temperature range yielded a value for ΔH^\ddagger ($19.0 \pm 0.5 \text{ kcal/mol}$), which is ca. 3 kcal higher than the corresponding value for **5.3** (16.2 kcal/mol). The ΔS^\ddagger values obtained for the two systems were roughly the same ($8.5 \pm 2.3 \text{ cal mol}^{-1} \text{ K}^{-1}$ for **19** compared to $3.6 \text{ cal mol}^{-1} \text{ K}^{-1}$).

A van't Hoff plot using the values of k_2 and k_{-2} from our kinetic simulations yielded a $\Delta H^\circ = 17.6 \text{ kcal/mol}$ and a $\Delta S^\circ = 80.4 \text{ cal mol}^{-1} \text{ K}^{-1}$ (Figure 5.19). Surprisingly, the exothermic ΔH° and large ΔS° differ significantly from the corresponding parameters derived by Piers.⁸ However, the equilibrium reaction presented in Figure 5.17 is fundamentally different from that proposed by Piers, and thus, should be expected to exhibit different thermodynamic parameters. The ΔS° value deserves further discussion as it is unusually large. While we do not currently have an explanation for a ΔS° of such magnitude, it is important to note that the primary purpose of the kinetic modeling was to obtain k_1 values and there is likely a large amount of error in the values of k_2 , k_{-2} , and k_3 (partly evidenced by the relatively poor linear fit in the van't Hoff plot). This being the case, we suspect that a more thorough modeling of the kinetic data would provide a more reasonable estimate of ΔS° .

Although we urge caution in extrapolating these results to behavior under

catalytic conditions and normal operating temperatures, this fundamental transformation in the RCM cycle is clearly much more difficult for **5.19** compared to **5.3**, and may partially explain the lower activities typically associated with complexes of this type. Furthermore, since loss of the cyclopentene product from **5.19** or **5.4** appears to be the rate-determining step in the ring-closing direction, we speculate that the relative increase in the height of this barrier for **5.19** may allow for more degenerate turnovers to occur before a productive turnover can be completed.⁸ This would account for the observation that catalysts containing structurally similar NHCs select for degenerate turnovers during RCM.¹ Finally, the observation of ¹³C-**5.1** in solution suggests that ring opening of the cyclopentene RCM product is facile, and perhaps that the kinetic preference of ring-closing over ring-opening is catalyst dependent.²⁵

Conclusion and Future Outlook

In summary, several new phosphonium alkylidene ruthenium metathesis catalysts incorporating different NHCs have been prepared and used to generate ruthenacycles with the goal of rationalizing degenerate metathesis selectivity. In the case of ethylene-only ruthenacycles, the exchange rate of α and β methylene protons was found to vary considerably across the series of catalysts. With traditional NHCs, the exchange rate was largely consistent with previously reported complexes, while incorporation of a CAAC with DEP as the nitrogen substituent resulted in a severe attenuation of the exchange rate to the point where exchange was not observed until the temperature was increased to -30 °C. Due to this relatively slow exchange rate, one can envision that crystallographic characterization of this complex, or

analogous ones, may be possible. However, subtle changes in ligand architecture can alter the ruthenacycle exchange rate, and by extension, metathesis selectivity and activity. This was demonstrated by the remarkable increase in exchange rate upon substituting DEP with DIPP as the nitrogen substituent on the CAAC ligand. These results demonstrate the significant changes that can occur in even the simplest of metathesis reactions as a result of changes in the NHC structure.

Our attempts to form RCM-relevant ruthenacycles resulted in the formation of a previously unobserved ruthenacycle that we believe to be the first acyclic β -alkyl substituted ruthenacycle. Such a structure is consistent with all of our spectroscopic data, but its low concentration has placed a definitive identification currently out of our technical reach. Nevertheless, this structure plays an important role in ruthenacycle kinetics under an atmosphere of excess ethylene. Our kinetic investigations revealed that the rate-limiting dissociation of the cyclopentene RCM product from the ruthenium center has a much higher energy barrier compared to previously reported complexes. Considering that the majority of the steps along the RCM pathway appear to be reversible, this higher barrier may allow for more degenerate turnovers to occur at the expense of productive ones. At the very least, it provides additional rationale for the generally inferior performance of metathesis catalysts containing *N*-aryl/*N*-alkyl NHC's when compared to those possessing *N*-aryl/*N*-aryl NHCs.

Finally, these studies further illuminate the subtle role that the NHC plays in ruthenium catalyzed olefin metathesis, thus validating efforts to fine tune ruthenium catalysts for specific applications via manipulation of this ligand.

Experimental

General: All reactions were carried out in dry glassware under an argon atmosphere using standard Schlenk line techniques or in a Vacuum Atmospheres Glovebox under a nitrogen atmosphere unless otherwise specified. All solvents were purified by passage through solvent purification columns and further degassed with argon.²⁶ NMR solvents were dried over CaH_2 and vacuum transferred to a dry Schlenk flask and subsequently degassed with argon. Commercially available reagents were used as received unless otherwise noted.

Standard NMR spectroscopy experiments were conducted on a Varian Inova 400 MHz spectrometer, while VT and kinetic experiments were conducted on a Varian 500 MHz spectrometer equipped with an AutoX probe. Accurate temperature measurements of the NMR probe were obtained using a thermocouple connected to a multimeter with the probe immersed in an NMR tube containing a minimal amount of methylene chloride. Experiments and pulse sequences from Varian's Chempack 4 software were used. Chemical shifts are reported in ppm downfield from Me_4Si by using the residual solvent peak as an internal standard. Spectra were analyzed and processed using MestReNova Ver. 7.²⁷ Linear fits and plots were created using OriginPro 8.1.

High-resolution mass spectrometry (HRMS) data was obtained on a JEOL MSRoute mass spectrometer using FAB+ ionization.

Preparation of 5.6: A 100 mL RB flask was charged with catalyst **5**² (0.734 g, 0.93 mmol) and pyridine (3.9 mL) was added under air. The solution changed in color from brown to green over a period of ca. 25 minutes at which point the stirring was

stopped and pentane was carefully layered over the pyridine solution. The flask was placed in a $-10\text{ }^{\circ}\text{C}$ freezer and allowed to stand overnight, at which point a green oil had crashed out. The solvent was decanted away and the green oil was washed with excess pentane, dried in vacuo, and used without further purification (0.611 g).

In a glovebox, the green oil from above (0.611 g) was dissolved in C_6H_6 (10 mL) and $\text{P}(i\text{Pr})_3$ (290 μL , 1.38 mmol) was added which caused an immediate color change from green to brown. The solution was stirred for 45 minutes, removed from the glovebox, and conc. in vacuo. The brown/red residue was loaded onto a silica gel column (ca. 70 mL) and flashed with 10% Et_2O /pentane, followed by 40% Et_2O /pentane. The pink/red band was collected and conc. to give **5.6** (0.403 g, 66%). ^1H NMR (400 MHz, C_6D_6) δ 19.45 (s, 1H), 8.04 (br s, 2H), 7.12 (m, 1H), 6.92 (m, 2H), 6.15(m, 2H), 4.16 (m, 2H), 3.11 (m, 4H), 2.59 (m, 3H), 2.27 (br s, 6H), 1.75 (m, 6H), 1.46 (m, 2H), 1.04 (d, $J = 7.3$ Hz, 9H), 1.01 (d, $J = 7.3$ Hz, 9H) 0.91 (t, $J = 7.4$ Hz, 3H). ^{13}C NMR (101 MHz, C_6D_6) δ 295.69, 219.78, 219.02, 151.56, 137.51, 137.38, 136.97, 130.99, 129.13, 50.89, 48.22, 48.19, 30.65, 22.47, 22.31, 21.04, 20.56, 19.64, 18.80, 14.43. ^{31}P NMR (162 MHz, C_6D_6) δ 41.39. HRMS (FAB+): Calculated—666.2219, Found—666.2235.

Preparation of 5.8: In a glovebox, a 100 mL RB flask was charged with **5.7**⁶ (0.108 g, 0.635 mmol) and **5.6** (0.403 g, 0.605 mmol). Methylene chloride (25 mL) was added and the solution was stirred for 14 h, after which it was concentrated inside the glovebox and carefully transferred to a sublimation apparatus. The sublimator was heated to $60\text{ }^{\circ}\text{C}$ under dynamic vacuum (10–100 mTorr) for 2 h. After cooling

to RT, the sublimator was placed back inside the glovebox, and the remaining yellow-brown residue was dissolved in a minimal amount of CH_2Cl_2 and transferred to a 20 mL scintillation vial where the solution was conc. to dryness. Pentane was added and the resulting suspension was stirred vigorously for 5 min after which the pentane was decanted away to yield **5.8** (0.193 g, 54%) as a yellow solid after drying. ^1H NMR (300 MHz, CD_2Cl_2) δ 6.94 (s, 2H), 3.91 (m, 4H), 3.49 (m, 2H), 2.67 (m, 3H), 2.31 (s, 6H), 2.28 (s, 3H), 1.75 (m, 2H), 1.36 (d, $J = 7.2$ Hz, 9H), 1.31 (d, $J = 7.2$ Hz, 9H), 1.24 (m, 2H), 0.96 (t, $J = 7.4$ Hz, 3H). ^{13}C NMR (101 MHz, C_6D_6) δ 471.37, 211.77, 210.93, 138.54, 138.15, 129.47, 51.78, 51.18, 51.15, 49.25, 49.21, 30.65, 22.91, 22.72, 21.40, 20.70, 19.78, 18.53, 14.36. ^{31}P NMR (121 MHz, CD_2Cl_2) δ 42.49. HRMS (FAB+): Calculated—589.1820, Found—589.1815.

Preparation of 5.9: In a glovebox, a Schlenk flask was charged with **5.8** (128 mg, 0.218 mmol) and CH_2Cl_2 (10 mL). The flask was sealed, removed from the glovebox, and HCl (1 M in Et_2O , 3.3 mL, 3.3 mmol) was added in one portion. The flask was sealed under argon and stirred for 16 h at RT, after which the solution was conc. and taken back into the glovebox. The yellow-brown residue was dissolved in a minimal amount of CH_2Cl_2 and transferred to a 20 mL scintillation vial where pentane was carefully layered on top. The vial was chilled to -35 °C overnight which resulted in the formation of yellow needle-like crystals that were isolated by decantation of the supernatant followed by washing with pentane. Drying of the washed crystals yielded **5.9** (109 mg, 81%). ^1H NMR (400 MHz, CD_2Cl_2) δ 19.36 (d, $J = 51.6$ Hz, 1H), 6.97 (s, 2H), 4.51 (m, 2H), 3.82 (m, 4H), 3.31 (dt, $J = 15.0, 7.4$ Hz, 3H), 2.32 (s, 3H), 2.19 (s, 6H), 1.88 (m, 2H), 1.55 (m, 2H), 1.21 (d, $J = 7.4$ Hz,

9H), 1.18 (d, $J = 7.3$ Hz, 9H), 1.04 (t, $J = 7.4$ Hz, 3H). ^{13}C NMR (151 MHz, CD_2Cl_2) δ 273.08, 200.80, 138.85, 138.07, 137.81, 130.41, 130.14, 52.84, 52.25, 48.23, 30.91, 25.60, 25.36, 21.31, 20.63, 18.19, 18.01, 17.99, 14.40. ^{31}P NMR (162 MHz, CD_2Cl_2) δ 39.86. HRMS (FAB+): Calculated—626.1479, Found—626.1482.

Preparation of 5.11: In a glovebox, a Schlenk flask was charged with **5.10a**¹⁴ (51 mg, 0.088 mmol), **5.7** (19 mg, 0.114 mmol), $\text{P}(\text{Pr})_3$ (24 μL , 0.114 mmol), and CH_2Cl_2 (2 mL). The flask was sealed, removed from the glovebox, and heated to 35 °C for 2 h. During this period, a color change from green to light yellow occurred. After cooling to RT, the solution was conc., taken back into the glovebox, and transferred to a sublimation apparatus where it was worked up in an analogous manner to compound **5.8**. After removal from the sublimator, the brown-yellow residue was washed with pentane and dried to give **5.11** (12 mg). Chilling the pentane wash to -35 °C for several hours provided an additional crop of **5.11** (19 mg, 31 mg total, 59%). ^1H NMR (400 MHz, CD_2Cl_2) δ 7.31 (m, 3H), 2.83 (m, 2H), 2.72 (d, 3H), 2.53 (m, 2H), 2.09 (s, 2H), 1.72 (s, 6H), 1.36 (s, 6H), 1.34 (d, $J = 7.6$ Hz, 9H), 1.31 (d, $J = 7.6$ Hz, 9H), 1.17 (t, $J = 7.2$ Hz, 6H). ^{13}C NMR (151 MHz, CD_2Cl_2) δ 474.27, 266.11, 265.60, 142.84, 139.82, 139.80, 129.17, 126.69, 80.96, 80.94, 58.68, 58.64, 52.50, 52.48, 31.18, 29.09, 25.43, 22.41, 22.29, 19.76, 14.78. ^{31}P NMR (162 MHz, CD_2Cl_2) δ 40.50. HRMS (FAB+): Calculated—601.1945, Found—601.1967.

Preparation of 5.13: In a glovebox, a Schlenk flask was charged with **5.11** (12 mg, 0.019 mmol) and CH_2Cl_2 (1 mL). The flask was sealed, removed from the box, and $\text{HBF}_4\text{-Et}_2\text{O}$ (5 μL , 0.037 mmol) was added in one portion. After stirring at RT for 1.5 h, the solution was conc. and taken back into the box where the crude product

was vigorously washed with pentane and dried to give **5.13** (12 mg, 91% yield). ^1H NMR (400 MHz, CD_2Cl_2) δ 17.28 (d, $J = 34.8$ Hz, 1H), 7.66 (t, $J = 7.2$ Hz, 1H), 7.52 (d, $J = 8.0$ Hz, 2H), 2.81–2.73 (m, 3H), 2.62–2.55 (m, 2H), 2.37 (s, 2H), 2.32–2.26 (m, 2H), 1.98 (s, 6H), 1.41 (s, 6H), 1.19 (d, $J = 7.6$ Hz, 6H), 1.16–1.13 (m, 18H). ^{13}C NMR (101 MHz, CD_2Cl_2) δ 265.41, 263.52 (d, $J = 21.3$ Hz), 247.31, 141.66, 136.88, 130.61, 128.16, 127.41, 82.02, 55.58, 52.02, 51.48, 28.69 (q, $J = 27.33$), 25.32, 25.06, 24.67, 24.46, 24.02, 21.70, 21.30, 21.12, 20.75, 17.41 (q, $J = 33.2$ Hz), 13.43 (q, $J = 32.5$ Hz). ^{31}P NMR (121 MHz, CD_2Cl_2) δ 59.01 (d, $J = 19.2$ Hz). HRMS (FAB+): Calculated—602.2024, Found—602.2005.

Preparation of 5.12: In a glovebox, a Schlenk flask was charged with **5.10b**¹⁴ (167 mg, 0.276 mmol), **5.7** (61 mg, 0.359 mmol), $\text{P}(\text{iPr})_3$ (68 μL , 0.359 mmol) and C_6H_6 (ca. 4 mL). The flask was sealed, removed from the glovebox, and heated to 80 °C until complete conversion of the starting material (monitored by ^1H NMR spectroscopy, ca. 30 h). After cooling to RT, the reaction was conc. and transferred to a sublimation apparatus inside the glovebox and worked up as above. After removal from the sublimator, the brown-yellow residue was vigorously stirred with pentane for 5 min after which the solvent was removed by decantation and the resulting yellow solid dried to give **5.12** (126 mg, 72%). ^1H NMR (500 MHz, C_6D_6) δ 7.18–7.08 (m, 3H), 3.24 (sept, $J = 6.5$ Hz, 2H), 2.80–2.53 (m, 3H), 1.90 (s, 6H), 1.64 (s, 2H), 1.56 (d, $J = 6.3$ Hz, 6H), 1.24 (m, 24H), 1.01 (s, 6H). ^{13}C NMR (126 MHz, C_6D_6) δ 471.88, 268.01, 267.38, 147.52, 136.80, 136.78, 129.67, 125.33, 79.45, 79.42, 58.37, 58.32, 51.99, 51.97, 30.62, 29.83, 28.92, 27.35, 24.62, 22.32, 22.18, 19.63. ^{31}P NMR (162 MHz, CD_2Cl_2) δ 39.66. HRMS (FAB+): Calculated—629.2258,

Found—629.2276.

Preparation of 5.14: In a glovebox, a Schlenk flask was charged with **5.12** (32 mg, 0.051 mmol) and CH_2Cl_2 (4 mL). The flask was sealed, removed from the box, and $\text{HBF}_4\text{-Et}_2\text{O}$ (7 μL , 0.051 mmol) was added which resulted in an immediate color change from orange to brown (Note: When HCl in Et_2O was added to **5.12**, only decomposition was observed). The reaction was stirred for 1 h at RT and conc. before being taken back into the glovebox. Pentane was added and the solution was stirred vigorously until the solution became clear, after which the pentane was removed by decantation, and the resulting solid was washed with additional aliquots of pentane and dried to give **5.14** (28 mg, 77%). ^1H NMR (500 MHz, CD_2Cl_2) δ 17.24 (d, $J = 36.6$ Hz, 1H), 7.67 (t, $J = 7.5$ Hz, 1H), 7.53 (d, $J = 7.8$ Hz, 2H), 2.86 (sept, $J = 7.0$ Hz, 2H), 2.76 (m, 3H), 2.38 (s, 2H), 1.98 (s, 6H), 1.46 (s, 6H), 1.28 (d, $J = 6.7$ Hz, 6H), 1.23 (d, $J = 7.3$ Hz, 9H), 1.19 (d, $J = 7.3$ Hz, 9H), 0.81 (d, $J = 6.6$ Hz, 6H). ^{13}C NMR (126 MHz, CD_2Cl_2) δ 246.96, 246.94, 147.28, 134.76, 131.49, 126.91, 82.33, 56.03, 56.00, 50.81, 34.10, 29.90, 28.70, 28.07, 26.65, 24.08, 22.31, 21.71, 21.41, 17.85, 17.82, 13.80. ^{31}P NMR (162 MHz, CD_2Cl_2) δ 59.5 (d, $J = 7.8$ Hz). HRMS (FAB+): Calculated—631.2415, Found—631.2441.

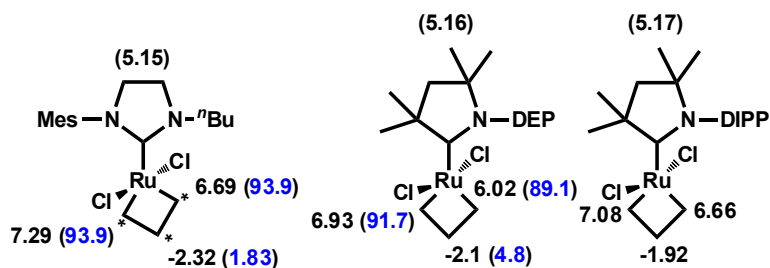


Figure 5.20. Ruthenacycle ^1H NMR and ^{13}C NMR (blue, where available) resonances for **5.15**, **5.16**, and **5.17**

General Procedure for Preparation of Ethylene-only Ruthenacycles (5.15, 5.16, and 5.17): In a glovebox, a 4 mL vial was charged with **9** (12 mg, 0.019 mmol) and $B(C_6F_5)_3$ (12 mg, 0.023 mmol, note that this reagent is not necessary for forming **16** and **17**). The contents of the vial were dissolved in CD_2Cl_2 (0.6 mL) and transferred to a J. Young NMR tube which was sealed, removed from the glovebox and cooled to $-78\text{ }^\circ\text{C}$ in a dry ice/acetone bath. The NMR tube was evacuated and ca. 1 atm of ethylene was added via balloon or through the vacuum manifold. The tube was shaken and then warmed to ca. $-40\text{ }^\circ\text{C}$ in a $CO_2/MeCN$ bath for 2-4 h after which the tube was cooled to $-78\text{ }^\circ\text{C}$ and taken to the NMR spectrometer for analysis. In general, we were only able to accurately assign the ^1H and ^{13}C resonances of the ruthenacycle protons and carbons as the ligand resonances appeared to be complicated by decomposition products. In the case of compound **17**, we were unable to obtain a clean ^{13}C NMR spectrum since the complete

Table 5.2. T_1 Values for catalysts **5.15**, **5.16**, and **5.17**

Complex	Temperature, $^\circ\text{C}$	T_1 , s
5.15	-50	0.271
5.15	-60	0.282
5.15	-70	0.296
5.15	-80	0.267
5.16	-30	0.242
5.17	-60	0.303

conversion of **14** to **17** was never achieved without significant decomposition.

Determination of Methylene Exchange Rates and Eyring Plot: The method used to measure the exchange rate of α and β methylene protons was the spin

saturation transfer method. This method entails the observation of one of the sites of an exchanging system while the other site is saturated with a selective inversion pulse. As a result of the chemical exchange, the intensity of the observed peak decreases until a new steady state is reached. The ratio of the intensity of this new steady-state resonance to the original peak intensity is related to the T_1 of the observed resonance and the rate of chemical exchange by Eq. 1.

$$M_{zA}(\infty) = M_{0A} \frac{T_A}{T_A + T_{1A}} \quad (1)$$

Rearranging Eq. 1 with $k_A = 1/T_A$ and $R_A = 1/T_{1A}$ yields Eq. 2.

$$\frac{M_{zA}(\infty)}{M_{0A}} = \frac{R_A}{R_A + k_A} \quad (2)$$

The T_1 s of the ruthenacycle peaks were measured using the inversion recovery method at the desired temperature.¹²

Ethylene-only ruthenacycles were prepared as described above and equilibrated to the desired temperature. The vNMRj PRESAT pulse sequence was used to selectively invert the downfield exchanging ruthenacycle peak ($\delta \approx 7$ ppm) and an array of delay times (satdly, 0.001 to 1.5 s in 0.1 s intervals) was set up in order to determine the steady state intensity of the peak under observation ($\delta \approx -2$ ppm).²⁸

The exchange rate was then calculated using Eq. 2.

General Procedure for Preparation of Substituted Ruthenacycles (5.15, 5.19, 5.22): In a glovebox, a 1 mL volumetric flask was charged with hexamethyldisiloxane (HMDSO, 28 mg, 0.170 mmol) and filled to the line with CD_2Cl_2 to create a 0.170 M solution of internal standard. A 4 mL vial was charged with 20 μ L of HMDSO stock

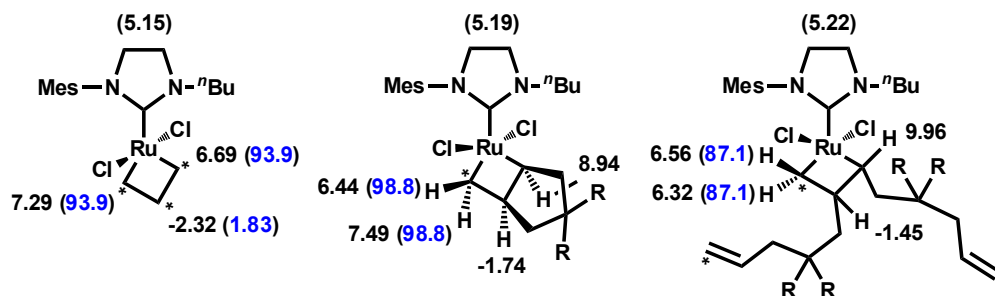


Figure 5.21. Ruthenacycle ^1H NMR and ^{13}C NMR (blue, where available) resonances for **5.15**, **5.19**, and **5.22** in CD_2Cl_2 .

solution and **5.17** (15 μL , 0.067 mmol). A separate 4 mL vial was charged with **5.9** (13 mg, 0.0214 mmol) and $\text{B}(\text{C}_6\text{F}_5)_3$ (13 mg, 0.026 mmol). Both vials were placed in the glovebox cold well which was packed with ChemGlass Lab Armor (CLS-2991-002) and cooled to between $-50\text{ }^\circ\text{C}$ and $-80\text{ }^\circ\text{C}$ using liquid nitrogen (alternatively, the glovebox freezer could be used). A separate vial containing CD_2Cl_2 and an empty J. Young NMR tube were also cooled to the same temperature. Chilled CD_2Cl_2 (0.6 mL) was added to the vial containing **5.9** and after mixing, the vial was placed back in the cold well for 30 min after which the catalyst solution was added to the vial containing **5.17** and the contents quickly transferred to the J. Young tube which was sealed, immediately removed from the glovebox and frozen in liquid nitrogen. After attaching to a high-vacuum manifold, the NMR tube was evacuated and ca. 1 eq. of ethylene was condensed into the tube via a calibrated gas bulb. The tube was carefully warmed to $-78\text{ }^\circ\text{C}$ and shaken several times before warming to $-40\text{ }^\circ\text{C}$ for 2–4 h. For NMR analysis, the tube was transported in a $-78\text{ }^\circ\text{C}$ bath before being placed into the spectrometer which was cooled to the desired temperature.

General Procedure for Kinetics of Conversion of 5.19 to 5.15: A mixture of **5.15**, **5.19**, and **5.22** in CD_2Cl_2 (0.6 mL) was prepared as described above and a spectrum was taken at the desired temperature to determine the initial concentrations of **5.15**, **5.19**, and **5.22**. The NMR tube was then removed from the spectrometer and cooled to $-78\text{ }^\circ\text{C}$ before being attached to a vacuum manifold where it was evacuated and backfilled with ca. 1 atm of ethylene. The tube was shaken and placed back inside the spectrometer and the kinetic run was started at the desired temperature. Spectra were recorded at periodic intervals by arraying the vNMRj 'pad' (pulse acquisition delay) function with a delay of 10 s between pulses. Kinetic runs conducted at $-60\text{ }^\circ\text{C}$ and $-55\text{ }^\circ\text{C}$ were generally too slow to obtain data over several half-lives of **5.19** (e.g., $t_{1/2} > 8\text{ h}$). In these cases, data was collected as long as was practical (ca. 8 h). At all other temperatures, kinetic data was collected for several half-lives of **5.19**.

Spectra were phased and baseline corrected prior to integration of the peaks corresponding to **5.15**, **5.19**, **5.22**, and HMDSO. At higher temperatures ($-40\text{ }^\circ\text{C}$ and $-45\text{ }^\circ\text{C}$), it became difficult to obtain accurate concentrations towards the end of the reaction, hence the large error in the concentration profiles of the reactions conducted at these temperatures.

Discussion of Kinetic Modeling: The experimental concentration profiles of **5.15**, **5.19**, and **5.22** were fitted using the Parameter Estimation function (Levenberg–Marquardt method) in COPASI 4.6 according to reaction sequence presented in Figure 5.17.²¹ Unfortunately, there are more reaction parameters than observable variables (e.g., the concentration of **5.1** could not be determined reliably during the reaction). Therefore, the model is a simplification of what is actually occurring and

any evaluation of the computed rate constants should take this fact into account. Nevertheless, kinetic fits were in generally good agreement with the experimental data (Figure S18).

The following variables were floated in order to allow COPASI to arrive at a solution: initial concentration of **5.15**, initial concentration of **5.19**, initiation concentration of **5.22**, k_1 , k_2 , k_{-2} , and k_3 . The initial concentrations of the ruthenacycle species were varied in order to obtain the best fit possible and were generally in good agreement with the experimentally determined concentrations.

References

- (1) Stewart, I. C.; Keitz, B. K.; Kuhn, K. M.; Thomas, R. M.; Grubbs, R. H. *J. Am. Chem. Soc.* **2010**, *132*, 8534.
- (2) Thomas, R. M.; Keitz, B. K.; Champagne, T. M.; Grubbs, R. H. *J. Am. Chem. Soc.* **2011**, *133*, 7490.
- (3) (a) Sanford, M. S.; Love, J. A.; Grubbs, R. H. *J. Am. Chem. Soc.* **2001**, *123*, 6543. (b) Love, J. A.; Sanford, M. S.; Day, M. W.; Grubbs, R. H. *J. Am. Chem. Soc.* **2003**, *125*, 10103.
- (4) (a) Hong, S. H.; Day, M. W.; Grubbs, R. H. *J. Am. Chem. Soc.* **2004**, *3*, 7414. (b) Courchay, F. C.; Sworen, J. C.; Ghiviriga, I.; Abboud, K. A.; Wagener, K. B. *Organometallics* **2006**, *25*, 6074. (c) Hong, S. H.; Wenzel, A. G.; Salguero, T. T.; Day, M. W.; Grubbs, R. H. *J. Am. Chem. Soc.* **2007**, *129*, 7961.
- (5) (a) Wenzel, A. G.; Grubbs, R. H. *J. Am. Chem. Soc.* **2006**, 16048. (b) Romero, P. E.; Piers, W. E. *J. Am. Chem. Soc.* **2007**, *129*, 1698. (c) Wenzel, A. G.; Blake,

- G.; VanderVelde, D. G.; Grubbs, R. H. *J. Am. Chem. Soc.* **2011**, *133*, 6249.
- (6) (a) Romero, P. E.; Piers, W. E.; McDonald, R. *Angew. Chem. Int. Ed.* **2004**, *43*, 6161. (b) Rowley, C. N.; Eide, E. F. van der; Piers, W. E.; Woo, T. K. *Organometallics* **2008**, *27*, 6043. (c) Eide, E. F. van der; Romero, P. E.; Piers, W. E. *J. Am. Chem. Soc.* **2008**, *130*, 4485. (d) Leitao, E. M.; Eide, E. F. van der; Romero, P. E.; Piers, W. E.; McDonald, R. *J. Am. Chem. Soc.* **2010**, *132*, 2784.
- (7) Ruthenacycles have been studied quite extensively in the gas phase, see : (a) Hinderling, C.; Adlhart, C.; Chen, P. *Angew. Chem. Int. Ed.* **1998**, *37*, 2685. (b) Adlhart, C.; Hinderling, C.; Baumann, H.; Chen, P. *J. Am. Chem. Soc.* **2000**, *122*, 8204.
- (8) Eide, E. F. van der; Piers, W. E. *Nature Chemistry*. **2010**, *2*, 571.
- (9) Although it would have been advantageous to access ruthenacycles directly from the bis-pyridine adduct of **5.5**, a technique demonstrated in ref. 5c, we found that such a complex could not be isolated as a single clean species. See the Experimental section.
- (10) Carlson, R. G.; Gile, M. A.; Heppert, J. A.; Mason, M. H.; Powell, D. R.; VanderVelde, D.; Vilain, J. M. *J. Am. Chem. Soc.* **2002**, *124*, 1580.
- (11) Keitz, B. K.; Grubbs, R. H. *J. Am. Chem. Soc.* **2011**, *133*, 16277.
- (12) Unfortunately, while the resonances corresponding to the ruthenacycle protons were well resolved, other ligand peaks could not be cleanly identified, most likely due to some decomposition taking place during the reaction as evidenced by the relatively low yield of ruthenacycle.
- (13) Sandström, J.; *Dynamic NMR Spectroscopy*, Academic Press Inc.: New York,

1982; pp. 53.

(14) Complete conversion to ruthenacycle **5.17** from **5.14** was never observed, even after extended periods of time at ca. $-40\text{ }^{\circ}\text{C}$. Attempts to raise the temperature resulted in decomposition of **5.17**.

(15) (a) Anderson, D. R. ; Lavallo, V.; O'Leary, D. J.; Bertrand, G.; Grubbs, R. H. *Angew. Chem. Int. Ed.* **2007**, *46*, 7262. (b) Anderson, D. R.; Ung, T. A.; Mkrtumyan, G.; Bertrand, G.; Grubbs, R. H.; Schrodi, Y. *Organometallics*. **2008**, *27*, 563.

(16) The low yielding synthesis of catalysts of type **5.10** hampered our ability to exhaustively examine the behavior of **5.13** and **5.14**.

(17) Several smaller peaks which could correspond to structural analogues of **5.4** are also visible in Figure 5.12. However, due to the extremely low intensity of these resonances, we can only speculate about their identity.

(18) Roberts, J. *ABCs of FT-NMR*, University Science Books : Sausalito, California, 2000; p. 61.

(19) The presence of $^{13}\text{C-1}$ was also confirmed by HRMS (FAB+). Calculated—242.1429, Found—242.1471 after warming the reaction to RT.

(20) Another structure consistent with all of the spectroscopic data is an isomer of **5.19**. However, the large differences in the reactivity of **5.19** and **5.22** with excess ethylene leads us to believe that this is probably not the case.

(21) Direct conversion of **5.22** into **5.15** would require generation of a ruthenium methylidene (**5.21**) and the release of **5.23** (dashed arrows in Figure 5.14). However, neither species was detected by ^1H NMR spectroscopy or HRMS, suggesting that **5.22** prefers to give an alkylidene which subsequently reacts with ethylene to give

5.15.

(22) COPASI (Complex Pathway Simulator) Hoops, S.; Sahle, S.; Gauges, R.; Lee, C.; Pahle, J.; Simus, N.; Singhal, M.; Xu, L.; Mendes, P.; Kummer, U. *Bioinformatics* **2006**, *22*, 3067.

(23) Notably, our model does not rely on the positive identification of **5.22**, but only that there is some equilibrium involving **5.19** and another ruthenacycle complex.

(24) At longer reaction times, where the change in concentration of **22** is relatively insignificant and the primary reaction consuming **5.19** is k_1 , the k_{obs} values from a log plot and k_1 values obtained from modeling were generally in good agreement (within a factor of 2 or less).

(25) For a discussion on the kinetic favorability of ring-closing, see ref. 8.

(26) Love, J.A.; Morgan, J.P.; Trnka, T.M.; Grubbs, R.H., *Angew. Chem. Int. Ed.* **2002**, *41*, 4035.

(27) www.mestrelab.com

(28) In principle, it is also possible to obtain the same rate by irradiating the downfield resonance and observing the upfield resonance. However, we found it easier to observe the downfield resonance as it is far removed from any overlapping peaks.